Dissipative Control of Energy Flow in Interconnected Systems

Y. Kishimoto[1] AND D. S. Bernstein[2]
University of Michigan, Ann Arbor, MI

S. R. Hall[3]
Massachusetts Institute of Technology, Cambridge, MA

Abstract

Dissipative energy flow controllers are designed for interconnected modal subsystems. Active feedback controllers for vibration suppression are then viewed as either an additional subsystem or a dissipative coupling. These controllers, which are designed by the LQG positive real control approach, maximize energy flow from a specified modal subsystem.

1. Introduction

Energy flow has been widely studied as an effective tool for analyzing large, interconnected vibrating systems. One of the key results of this approach is the fact that, within interconnected subsystems, energy flow can often be expressed as a linear combination of subsystem energy.

In active control for reducing vibration, energy flow has been considered as a performance index to be minimized [1]-[6]. The design of these active controllers, however, has some difficulties. For example, the optimal controller is often noncausal [5] and thus asymptotic stability of the closed-loop system cannot be guaranteed. Furthermore, active energy flow control for interconnected structures composed of more than two subsystems has received limited attention due to the lack of energy flow models for such interconnected systems.

In recent work [7, 8] motivated by Wyatt *et al.* [9] an energy flow model was derived for a structure consisting of several modal subsystems that are coupled either conservatively or dissipatively. In the present paper, our goal is to design active control laws for coupled subsystems by applying these energy flow models.

Three typical situations requiring energy flow controllers are considered in this paper. First, in Section 4, we consider energy flow control for several subsystems interconnected by conservative coupling [7]. For such an interconnected system, the control law can be designed for the system as a whole, which requires an energy flow model for the entire system including the controller. We thus treat the controller as an additional subsystem interconnected by a conservative coupling, so that energy flow is controlled through the coupling.

Next, in Section 5, we consider energy flow control among individual structural modes. Here we exploit the fact that structural modes are essentially coupled by the input and output matrices. By appropriately enlarging the input and output matrices, we design a dissipative controller that serves, in effect, as a dissipative coupling [8]. As an application of this approach, in Section 6 we consider two uncoupled systems that are controlled by a relative force.

In both cases the controller is designed to maximize the steady state energy flow from one of the subsystems, so that we can reduce the vibration of the specified subsystem. The control approach we use is due to Lozano-Leal and Joshi [10]. This approach is briefly reviewed in Section 3. Since the controller and plant are both positive real, closed-loop asymptotic stability is guaranteed in spite of modeling uncertainty.

2. Energy Flow Model for Interconnected Systems

In this section we briefly review some results concerning energy flow obtained in [7]-[9]. Consider r subsystems $z_1(s), \ldots, z_r(s)$ interconnected by a linear time-invariant coupling $L(s)$. Each subsystem $z_i(s)$ is assumed to be a strictly positive real and thus asymptotically stable scalar transfer function. Now we define normalized white noise $\tilde{w}(t) \triangleq [\tilde{w}_1(t) \cdots \tilde{w}_n(t)]^{\mathrm{T}}$ whose intensity matrix is identity. Assume that the disturbance vector $w_0(t) \triangleq [w_1(t) \cdots w_r(t)]^{\mathrm{T}}$ is now given by

$$w_0(t) = D\tilde{w}(t), \tag{1}$$

where $D \in \mathcal{R}^{r \times n}$ is the constant matrix, then the intensity matrix $S_{w_0 w_0}$ of $w_0(t)$ is given by $S_{w_0 w_0} = DD^{\mathrm{T}}$.

For later use, define $r \times r$ diagonal transfer function

$$Z(s) \triangleq \operatorname{diag}(z_1(s), z_2(s), \ldots, z_r(s)). \tag{2}$$

By defining the r-dimensional vectors

$$u_0 \triangleq [u_1 \cdots u_r]^{\mathrm{T}},\ y_0 \triangleq [y_1 \cdots y_r]^{\mathrm{T}},\ v_0 \triangleq [v_1 \cdots v_r]^{\mathrm{T}},$$

we obtain the feedback representation of the interconnected system shown in Fig. 2.1 in terms of $Z^{-1}(s)$, which is strictly positive real, and where $v_0 = Ly_0$ and $u_0 = w_0 - v_0$.

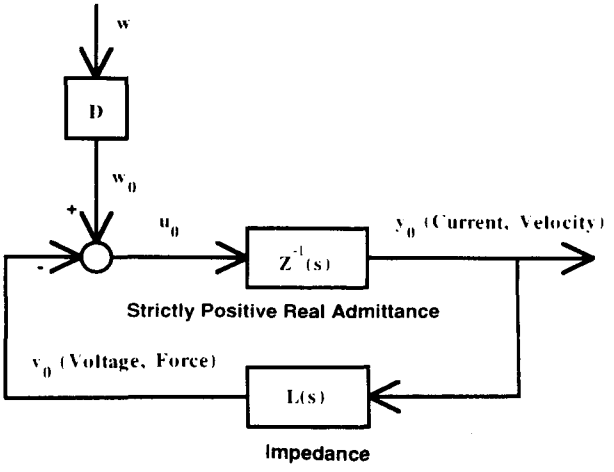

Fig. 2.1. Feedback Representation of Interconnected System.

[1]Graduate Student, Department of Aerospace Engineering
[2]Associate Professor, Department of Aerospace Engineering
[3]Associate Professor, Department of Aeronautics and Astronautics
Senior Member AIAA

We now introduce three steady state energy flows P_i^{p}, P_i^{d}, P_i^{e}, $i = 1, \ldots, r$,

P_i^{p} = the steady state average energy flow entering the ith subsystem through the ith port of $L(s)$,

P_i^{d} = the steady state average energy dissipation rate of the ith subsystem,

P_i^{e} = the steady state average external energy flow entering the ith subsystem.

Fig. 2.2 illustrates the resulting energy flow model for the case $r = 3$.

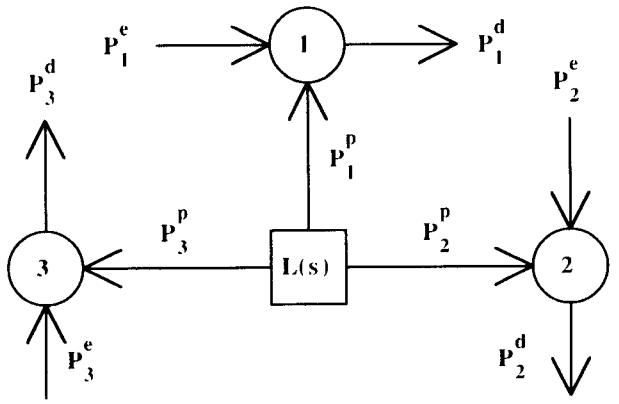

Fig. 2.2. Energy Flow Model with Three Subsystems.

Furthermore, these energy flows satisfy the conservation of energy, that is,

$$P_i^{\mathrm{p}} + P_i^{\mathrm{d}} + P_i^{\mathrm{e}} = 0, \quad i = 1, \ldots, r. \tag{3}$$

3. LQG Positive Real Control Approach

In this section we briefly review the LQG positive real control approach developed in [10].

The LQG control approach provides the optimal controller for the following problem. Given the nth-order stabilizable and detectable plant

$$\dot{x}(t) = Ax(t) + Bu(t) + D_1\tilde{w}(t), \tag{4}$$

$$y(t) = Cx(t) + D_2\tilde{w}(t), \tag{5}$$

determine an nth-order dynamic feedback compensator $G_{\mathrm{c}}(s) \sim \left[\begin{array}{c|c} A_{\mathrm{c}} & B_{\mathrm{c}} \\ \hline C_{\mathrm{c}} & 0 \end{array}\right]$ of the form

$$\dot{x}_{\mathrm{c}}(t) = A_{\mathrm{c}}x_{\mathrm{c}}(t) + B_{\mathrm{c}}y(t), \tag{6}$$

$$u(t) = C_{\mathrm{c}}x_{\mathrm{c}}(t), \tag{7}$$

such that the closed-loop system (4) - (7) with dynamics matrix

$$\tilde{A} \triangleq \left[\begin{array}{cc} A & BC_{\mathrm{c}} \\ B_{\mathrm{c}}C & A_{\mathrm{c}} \end{array}\right]$$

is asymptotically stable and the H_2 performance index

$$J(A_{\mathrm{c}}, B_{\mathrm{c}}, C_{\mathrm{c}}) = \lim_{t\to\infty} \mathcal{E}\{\frac{1}{t}\int_0^t [x^{\mathrm{T}}(s)R_1x(s) + u^{\mathrm{T}}(s)R_2u(s)]\,ds \tag{8}$$

$$= \|\tilde{G}(s)\|_2^2 \tag{9}$$

is minimized, where

$$\tilde{G}(s) \sim \left[\begin{array}{c|c} \tilde{A} & \tilde{D} \\ \hline \tilde{E} & 0 \end{array}\right]$$

is the closed-loop transfer function from the unit intensity white noise disturbance $\tilde{w}(t)$ to the performance variables $z(t) = E_1x(t) + E_2u(t)$ and where $\tilde{D} \triangleq \left[\begin{array}{c} D_1 \\ B_{\mathrm{c}}D_2 \end{array}\right]$, $\tilde{E} \triangleq [E_1 \quad E_2C_{\mathrm{c}}]$, $R_1 \triangleq E_1^{\mathrm{T}}E_1$, $R_2 \triangleq E_2^{\mathrm{T}}E_2 > 0$ and $E_1^{\mathrm{T}}E_2 = 0$. It is assumed that A, B, C, D_1 and E_1 satisfy (i) (A, B) and (A, D_1) are stabilizable, and (ii) (C, A) and (E_1, A) are detectable. Furthermore, for convenience, define $V_1 \triangleq D_1D_1^{\mathrm{T}}$, $V_2 \triangleq D_2D_2^{\mathrm{T}} > 0$, and assume that $D_1D_2^{\mathrm{T}} = 0$.

For this problem the optimal compensator $(A_{\mathrm{c}}, B_{\mathrm{c}}, C_{\mathrm{c}})$ is given by

$$A_{\mathrm{c}} = A - QC^{\mathrm{T}}V_2^{-1}C - BR_2^{-1}B^{\mathrm{T}}P, \tag{10}$$

$$B_{\mathrm{c}} = QC^{\mathrm{T}}V_2^{-1}, \tag{11}$$

$$C_{\mathrm{c}} = -R_2^{-1}B^{\mathrm{T}}P, \tag{12}$$

where Q and P are $n \times n$ nonnegative-definite matrices satisfying

$$AQ + QA^{\mathrm{T}} + V_1 - QC^{\mathrm{T}}V_2^{-1}CQ = 0, \tag{13}$$

$$A^{\mathrm{T}}P + PA + R_1 - PBR_2^{-1}B^{\mathrm{T}}P = 0. \tag{14}$$

Next we assume that the plant (4), (5) is positive real. For positive real plants a strictly positive real controller is desirable since the negative-feedback closed-loop system is guaranteed to be asymptotically stable [11]. The controller obtained above, however, is not necessarily strictly positive real. For this problem, Theorem 1 of [10] can be used to obtain an nth-order strictly positive real compensator $-G_{\mathrm{c}}(s) \sim \left[\begin{array}{c|c} A_{\mathrm{c}} & B_{\mathrm{c}} \\ \hline -C_{\mathrm{c}} & 0 \end{array}\right]$ that minimizes the H_2 performance index $J(A_{\mathrm{c}}, B_{\mathrm{c}}, C_{\mathrm{c}})$. Since the plant $G(s) \sim \left[\begin{array}{c|c} A & B \\ \hline C & 0 \end{array}\right]$ is positive real, there exists a positive-definite matrix Q_0 satisfying [12]

$$AQ_0 + Q_0A^{\mathrm{T}} = -LL^{\mathrm{T}}, \tag{15}$$

$$Q_0C^{\mathrm{T}} = B. \tag{16}$$

As shown in [10], if the LQG weights V_1, V_2, R_1, R_2 are chosen according to

$$V_1 = LL^{\mathrm{T}} + BR_2^{-1}B^{\mathrm{T}} > 0, \tag{17}$$

$$V_2 = R_2 > 0, \tag{18}$$

$$R_1 > C^{\mathrm{T}}V_2^{-1}C, \tag{19}$$

then the dynamic compensator $-G_c(s)$ given by (10), (11) and (12) is strictly positive real. With $-G_c(s)$, the negative feedback closed-loop system matrix $\tilde{A}$ is now asymptotically stable as explained above.

In the following sections we consider two types of energy flow control problems in which the plant is positive real. In each case we design positive real controllers by means of the above approach.

4. Design of an Energy Flow Controller as an Additional Interconnected Subsystem

In this section we consider a control problem involving $r-1$ subsystems $z_i(s)$ interconnected by a stiffness coupling. In this problem we assume that the controller $z_c(s)$ can interact with the subsystems only through additional coupling elements. Thus the controller can be treated as an additional rth subsystem. The transfer functions $Z_z^{-1}(s) = \mathrm{diag}(z_1^{-1}(s), \ldots, z_{r-1}^{-1}(s))$ and $z_c^{-1}(s)$ are assumed to be expressed by the state space models

$$\dot{x}_z(t) = A_z x_z(t) + B_z u_z(t), \tag{20}$$

$$y_z(t) = C_z x_z(t), \tag{21}$$

$$\dot{x}_c(t) = A_c x_c(t) + B_c y(t), \tag{22}$$

$$u(t) = C_c x_c(t), \tag{23}$$

respectively, where $x_z(t) \in \mathcal{R}^{n_z}$, $x_c(t) \in \mathcal{R}^{n_c}$, $y_z(t) \in \mathcal{R}^{r-1}$, $u_z(t) \in \mathcal{R}^{r-1}$ and $y(t)$, $u(t)$ are scalars. As shown in Fig. 4.1, $Z^{-1}(s)$ in Fig. 2.1 is now comprised of both $Z_z^{-1}(s)$ and $z_c^{-1}(s)$, that is, $Z(s) = \mathrm{diag}[z_1(s), \ldots, z_{r-1}(s), z_c(s)]$, so that the total number of subsystems is r. Furthermore, $y_0(t)$ and $u_0(t)$ in Fig. 4.1 are given by

$$y_0 = \begin{bmatrix} y_z \\ u \end{bmatrix}, \qquad u_0 = \begin{bmatrix} u_z \\ y \end{bmatrix}.$$

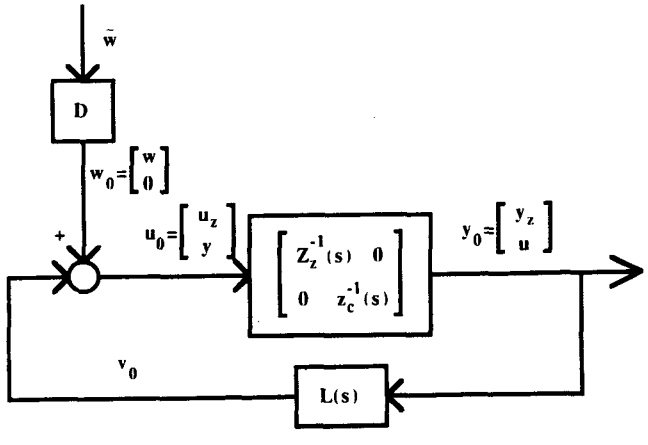

Fig. 4.1. Feedback Representation of Plant and Controller.

We now assume that the disturbance matrix $D \in \mathcal{R}^{r \times n}$ in Fig. 2.1 is the square matrix given by

$$D \triangleq \begin{bmatrix} D_{11} & 0 \\ 0 & 0 \end{bmatrix},$$

where $D_{11} \in \mathcal{R}^{(r-1)\times(r-1)}$. This assumption for D can be interpreted as that the disturbance $w_i(t), i = 1, \ldots, r-1$, is entering $z_i^{-1}(s)$, whereas no disturbance enters directly into the controller $z_c^{-1}(s)$. Thus $w_0(t)$ is now given by $w_0(t) = [w^{\mathrm{T}}(t)\ 0]^{\mathrm{T}}$, where $w(t) \triangleq [w_1(t) \cdots w_{r-1}(t)]^{\mathrm{T}}$. Since $u_0(t) = w_0(t) - v_0(t)$ it follows that

$$u_0 = \begin{bmatrix} u_z \\ y \end{bmatrix} = \begin{bmatrix} w(t) \\ 0 \end{bmatrix} - v_0(t),$$

which implies that $u_z(t)$ is the force vector resulting from the difference of the disturbance forces and the coupling forces, while $y(t)$ represents the coupling force only as shown in Fig. 4.1.

After the controller is connected, the stiffness coupling $L(s)$ is given by

$$L(s) = \frac{1}{s} C_L, \tag{24}$$

where the $r \times r$ symmetric matrix C_L is partitioned as

$$C_L \triangleq \begin{bmatrix} C_{L11} & C_{L12} \\ C_{L12}^{\mathrm{T}} & C_{L22} \end{bmatrix}, \tag{25}$$

and $C_{L11} \in \mathcal{R}^{(r-1)\times(r-1)}$.

We now assume that x_z in (20) consists of both positions and velocities so that there exists an output matrix C_p such that

$$\int y_z dt = C_p x_z. \tag{26}$$

Since $v_0 = L(s) y_0 = \frac{1}{s} C_L y_0$, it follows that

$$v_0 = C_L \int y_0 dt = C_L \begin{bmatrix} \int y_z dt \\ \int u dt \end{bmatrix} = C_L \begin{bmatrix} C_p x_z \\ x_{pc} \end{bmatrix}, \tag{27}$$

where a scalar state $x_{pc}(t)$ is defined by

$$\dot{x}_{pc}(t) \triangleq u(t). \tag{28}$$

From (20)-(23) and (27) the feedback system in Fig. 4.1 is given by

$$\dot{\tilde{x}}(t) = \tilde{A}\tilde{x}(t) + \tilde{D}\tilde{w}(t), \tag{29}$$

where

$$\tilde{x}(t) \triangleq \begin{bmatrix} x_z(t) \\ x_{pc}(t) \\ x_c(t) \end{bmatrix}, \quad \tilde{A} \triangleq \begin{bmatrix} A_z - B_z C_{L11} C_p & -B_z C_{L12} & 0 \\ 0 & 0 & C_c \\ -B_c C_{L12}^{\mathrm{T}} C_p & -B_c C_{L22} & A_c \end{bmatrix},$$

$$\tilde{D} \triangleq \begin{bmatrix} B_z D_{11} & 0 \\ 0 & 0 \\ 0 & 0 \end{bmatrix}.$$

We now wish to determine A_c, B_c and C_c in (22) and (23) by means of the LQG positive real approach described in Section 3. By defining

$$A \triangleq \begin{bmatrix} A_z - B_z C_{L11} C_p & -B_z C_{L12} \\ 0 & 0 \end{bmatrix}, \quad B \triangleq [0 \cdots 0 \ 1]^T,$$

$$C \triangleq [-C_{L12}^T C_p \ \ -C_{L22}], \quad D_1 \triangleq \begin{bmatrix} B_z D_{11} & 0 \\ 0 & 0 \end{bmatrix},$$

then $\tilde{A}$ and $\tilde{D}$ in (29) can be written as

$$\tilde{A} = \begin{bmatrix} A & BC_c \\ B_c C & A_c \end{bmatrix}, \quad \tilde{D} = \begin{bmatrix} D_1 \\ 0 \end{bmatrix}.$$

Thus by viewing (A, B, C) as a realization of the plant given by (4) and (5), (29) can be interpreted as an LQG control problem. As in Section 3 we consider the performance variables

$$z(t) = E_1 x(t) + E_2 u(t), \tag{30}$$

where $x(t) \triangleq \begin{bmatrix} x_z(t) \\ x_{pc}(t) \end{bmatrix}$ and $u(t)$ in (23) is the controller output to be included in the cost function.

The controller is now required to minimize the energy flow into the ith subsystem, that is, to minimize P_i^p. By defining

$$C_1 \triangleq \begin{bmatrix} C_z & 0 & 0 \\ 0 & 0 & C_c \end{bmatrix} \in \mathcal{R}^{r \times 2(n_z + n_L)},$$

P_i^e is given by [7]

$$P_i^e = \frac{1}{2}[D\tilde{D}^T C_1^T]_{(i,i)}. \tag{31}$$

Thus P_i^e is constant and independent of the controller gains. It thus follows from (3) that minimizing P_i^p is equivalent to minimizing $-P_i^d$.

To express the dissipation of the ith subsystem P_i^d in terms of the steady state covariance $\tilde{Q} \triangleq \lim_{t\to\infty} \mathcal{E}[x(t)x^T(t)]$, we now assume that each subsystem $z_i(s)$ has constant real part c_i and define

$$C_d \triangleq \mathrm{diag}(c_1, \ldots, c_{r-1}, 0) \in \mathcal{R}^{r \times r}, \tag{32}$$

then P_i^d, $i = 1, \ldots, r-1$, can be obtained by [7]

$$P_i^d = -[C_d C_1 \tilde{Q} C_1^T]_{(i,i)}, \tag{33}$$

where $\tilde{Q}$ satisfies the Lyapunov equation

$$0 = \tilde{A}\tilde{Q} + \tilde{Q}\tilde{A}^T + \tilde{D}\tilde{D}^T. \tag{34}$$

Thus the cost $-P_i^d$ to be minimized is given by

$$-P_i^d = [C_d C_1 \tilde{Q} C_1^T]_{(i,i)}. \tag{35}$$

Now using the definition of $\tilde{Q}$ yields

$$\begin{aligned} -P_i^d &= [C_d C_1 (\lim_{t\to\infty} \mathcal{E}[x(t)x^T(t)]) C_1^T]_{(i,i)} \\ &= \lim_{t\to\infty} \mathcal{E}[e_i^T C_d C_1 x(t) x^T(t) C_1^T e_i] \\ &= \lim_{t\to\infty} \mathcal{E}[\mathrm{tr}[x^T(t) C_1^T e_i e_i^T C_d C_1 x(t)]] \\ &= \lim_{t\to\infty} \mathcal{E}[x^T(t) C_1^T e_i c_i e_i^T C_1 x(t)]. \end{aligned}$$

Thus, letting the performance matrix E_1 in (30) be given by

$$E_1 = \sqrt{c_i} e_i^T C_1 \tag{36}$$

corresponds to minimizing $-P_i^d$.

As an illustrative numerical example we consider the three coupled oscillator system with controller as shown in Fig. 4.2, where $k_1 = 3.5$, $k_2 = 2.5$, $k_3 = 1$, $m_1 = 1$, $m_2 = 2$, $m_3 = 3$, $K_{12} = 0.5$, $K_{13} = 0.6$, $K_{23} = 0.7$, $K_{1c} = 0.8$, $K_{2c} = 0.9$, $K_{3c} = 1.0$ and $c_1 = 0.1$, $c_2 = 0.2$, $c_3 = 0.3$. Furthermore, let the white noise disturbances $w_i(t), i = 1, 2, 3$, have unit intensity $S_{w_i w_i} = 1$, that is, $D = \mathrm{diag}[1, 1, 1, 0]$. To maximize $-P_i^p$, $i = 1, 2, 3$, we set $E_2 = 0.1$ in (30). The resulting energy flow diagrams calculated by means of the steady state covariance [7] are illustrated in Fig. 4.3, where OL denotes the open-loop system and G_{c1}, G_{c2} and G_{c3} represent the controllers designed to maximize $-P_1^p$, $-P_2^p$ and $-P_3^p$, respectively. Fig. 4.3 shows that the controller absorbs energy from all of the subsystems and reduces the energy dissipation from each subsystem. Furthermore, it can be seen that the controller G_{ci} maximizes energy flow from the ith subsystem, that is, minimizes the energy dissipated by the specified subsystem.

To examine the actual reduction of vibration by these controllers, we define the steady-state stored energy by

$$\mathcal{E}_i \triangleq \frac{1}{2} m_i \mathcal{E}[\dot{x}_i^2(t)] + \frac{1}{2} k_i \mathcal{E}[x_i^2(t)], \quad i = 1, 2, 3, \tag{37}$$

where $x_i(t)$ and $\dot{x}_i(t)$ are the displacement and the velocity of the ith oscillator, respectively. Table 4.1 shows that each controller G_{ci} successfully reduces the stored energy $\mathcal{E}_i$ of the corresponding ith oscillator. For example, controller G_{c1} reduces the stored energy of oscillator 1 to 48.32 percent of its open-loop value.

Bode gain and phase plots of the controllers are shown in Fig. 4.4, which shows that the gain plot of controller G_{c1} has a peak near the coupled natural frequency of oscillator 1, that is, $\omega_1 = (k_1 + k_{12} + k_{13} + k_{1c})/m_1 = 2.3238$ (rad/sec). Similarly,

controller G_{c2} has a gain peak near $\omega_2 = 1.516$ (rad/sec), while controller G_{c3} has a gain peak near $\omega_3 = 1.048$ (rad/sec). These controllers are strictly positive real since their phase plots lie in the range $(-90°, 90°)$.

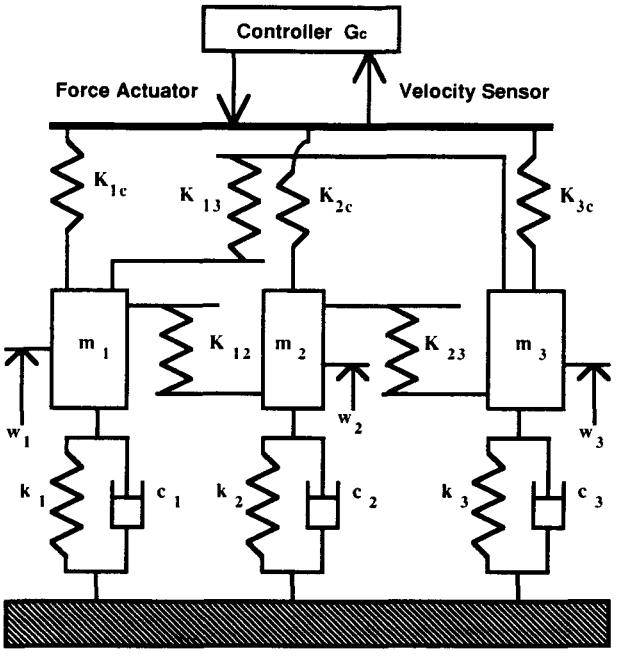

Fig. 4.2. Coupled Oscillator System with Controller.

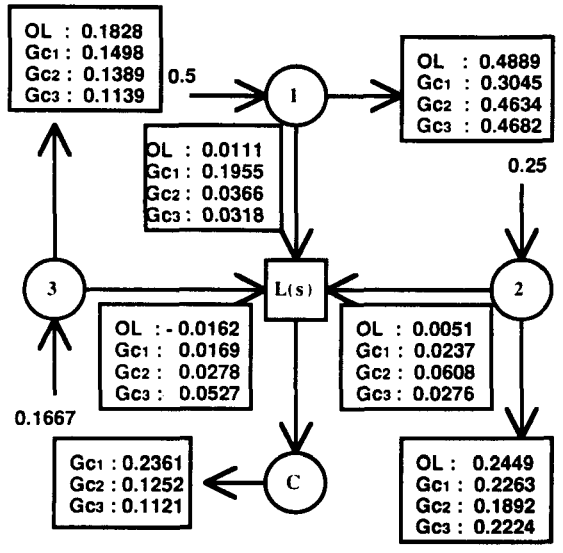

Fig. 4.3. Energy Flow among Oscillators for the Open-Loop System and for the Closed-Loop System with Controllers.

Stored Energy	Open-Loop	Controller 1	Controller 2	Controller 3
$\mathcal{E}_1$	4.2936	2.0747 (48.32%)	3.5476 (82.63%)	3.8208 (88.99%)
$\mathcal{E}_2$	2.0556	1.5775 (76.74%)	0.9772 (47.54%)	1.6290 (79.25%)
$\mathcal{E}_3$	1.3458	0.8542 (63.47%)	0.7809 (58.02%)	0.6374 (42.24%)

Table 4.1. Steady-State Stored Energy for Three Coupled Oscillators.

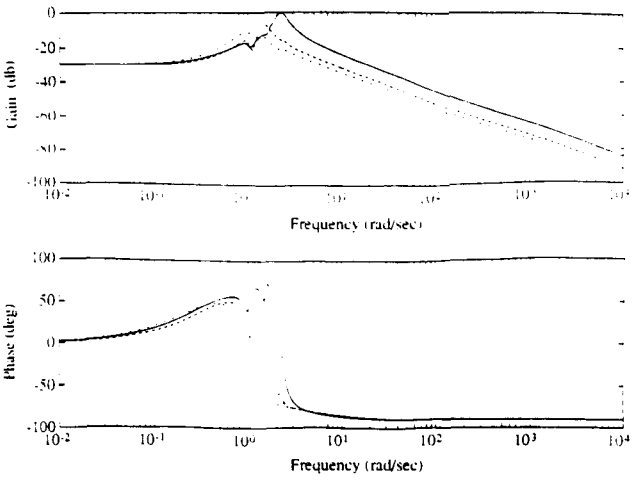

Fig. 4.4. Magnitude and Phase of Controllers G_{c1}(solid), G_{c2}(dashed), G_{c3}(dash-dot).

5. Design of an Energy Flow Controller as a Dissipative Coupling

In the previous section, we considered the subsystem interconnection explicitly in the energy flow analysis. As an alternative approach, we view the structure as a collection of uncoupled subsystems, such as modes, which become coupled only by means of the feedback controller. In contrast to the previous section, in which the control is applied to the flexible structure only through the conservative coupling, we now assume that the control force can be applied to the structure directly and design a controller to regulate energy flow among structural modes.

Consider a structure subject to unit intensity white noise disturbances $\tilde{w}_i(t)$, $i = 1, \ldots, n$, applied at locations ξ_{d_i}. The ith actuator located at ξ_i, $i = 1, \ldots, m$, applies a control force $u_i(t)$. Our goal is to design a controller that maximizes energy flow from the ith structural mode. For this purpose we consider each mode as a subsystem to obtain the feedback system corresponding to Fig. 2.1 and design a dissipative controller as a dissipative coupling.

First we denote the modal decomposition of the structure by

$$\eta(\xi, t) = \sum_{i=1}^{\infty} q_i(t)\psi_i(\xi), \tag{38}$$

where $q_i(t)$ denotes modal coordinates and $\psi_i(\xi)$ denotes orthogonal eigenfunctions. Then, using the boundary conditions and orthogonality properties, it follows that the modal coordinates $q_j(t)$ satisfy

$$\ddot{q}_j(t) + 2\zeta_j\omega_j q_j(t) + \omega_j^2 q_j(t) = \sum_{l=1}^{m} \psi_j(\xi_l)u_l(t) + \sum_{l=1}^{n} \psi_j(\xi_{d_l})\tilde{w}_l(t), \tag{39}$$

where we assume proportional damping $2\zeta_j\omega_j$. From (38), $\dot{\eta}(\xi_i,t)$ is the velocity of the structure at the ith actuator position ξ_i and we assume that m velocity sensors are also located at these positions. Hence the sensors and actuators are colocated and dual.

Now we consider r structural modes and define

$$\begin{aligned} x(t) &\triangleq [q_1(t)\ \dot{q}_1(t)\ q_2(t)\ \dot{q}_2(t)\ \cdots\ q_r(t)\ \dot{q}_r(t)]^{\mathrm{T}}, \\ u(t) &\triangleq [u_1(t)\ u_2(t)\ \cdots\ u_m(t)]^{\mathrm{T}}, \\ \tilde{w}(t) &\triangleq [\tilde{w}_1(t)\ \tilde{w}_2(t)\ \cdots\ \tilde{w}_n(t)]^{\mathrm{T}}, \\ y(t) &\triangleq [\dot{\eta}(\xi_1,t)\ \dot{\eta}(\xi_2,t)\ \cdots\ \dot{\eta}(\xi_r,t)]^{\mathrm{T}}. \end{aligned}$$

Then from (38) we obtain the state space model

$$\dot{x}(t) = Ax(t) + Bu(t) + D\tilde{w}(t), \tag{40}$$

$$y(t) = B^{\mathrm{T}}x(t), \tag{41}$$

where

$$A \triangleq \underset{i=1,\ldots,r}{\text{block}-\text{diag}} \begin{bmatrix} 0 & 1 \\ -\omega_i^2 & -2\zeta_i\omega_i \end{bmatrix} \in \mathcal{R}^{2r\times 2r},$$

$$B \triangleq \begin{bmatrix} 0 & \cdots & 0 \\ \psi_1(\xi_1) & \cdots & \psi_1(\xi_m) \\ 0 & \cdots & 0 \\ \psi_2(\xi_1) & \cdots & \psi_2(\xi_m) \\ \vdots & \vdots & \vdots \\ \vdots & \vdots & \vdots \\ 0 & \cdots & 0 \\ \psi_r(\xi_1) & \cdots & \psi_r(\xi_m) \end{bmatrix}, \quad D \triangleq \begin{bmatrix} 0 & \cdots & 0 \\ \psi_1(\xi_{d_1}) & \cdots & \psi_1(\xi_{d_n}) \\ 0 & \cdots & 0 \\ \psi_2(\xi_{d_1}) & \cdots & \psi_2(\xi_{d_n}) \\ \vdots & \vdots & \vdots \\ \vdots & \vdots & \vdots \\ 0 & \cdots & 0 \\ \psi_r(\xi_{d_1}) & \cdots & \psi_r(\xi_{d_n}) \end{bmatrix},$$

and $B \in \mathcal{R}^{2r\times m}$ and $D \in \mathcal{R}^{2r\times n}$.

To obtain the feedback system equivalent to Fig. 2.1 we introduce the diagonal matrix B_0 defined by

$$B_0 \triangleq \mathrm{diag}(0,1,0,1,\ldots,0,1) \in \mathcal{R}^{2r\times 2r},$$

and define

$$Z^{-1}(s) \sim \left[\begin{array}{c|c} A & B_0 \\ \hline B_0 & 0 \end{array}\right], \tag{42}$$

$$y_0(t) \triangleq B_0x(t) \in \mathcal{R}^{2r}, \tag{43}$$

$$w_0(t) \triangleq D\tilde{w}(t) \in \mathcal{R}^{2r}, \tag{44}$$

$$v_0(t) \triangleq -Bu(t) \in \mathcal{R}^{2r}. \tag{45}$$

We thus obtain Fig. 5.1 where the coupling $L(s)$ is defined by

$$L(s) \triangleq -BG_{\mathrm{c}}(s)B^{\mathrm{T}}. \tag{46}$$

Now using the LQG positive real approach we design a strictly positive real controller $G_{\mathrm{c}}(s)$ satisfying

$$G_{\mathrm{c}}(s) + G_{\mathrm{c}}^*(s) < 0,\ \mathrm{Re}[s] > 0, \tag{47}$$

so that $L(s)$ satisfies

$$\begin{aligned} L(s) + L^*(s) &= -BG_{\mathrm{c}}(s)B^{\mathrm{T}} - [BG_{\mathrm{c}}(s)B^{\mathrm{T}}]^* \\ &= -B[G_{\mathrm{c}}(s) + G_{\mathrm{c}}^*(s)]B^{\mathrm{T}} \\ &\geq 0, \end{aligned} \tag{48}$$

for $\mathrm{Re}[s] > 0$. Thus the coupling $L(s)$ serves as a dissipative controller which controls the energy flow among the structural modes. Our goal is to design $G_{\mathrm{c}}(s)$ so that $L(s)$ maximizes energy flow from a specified mode.

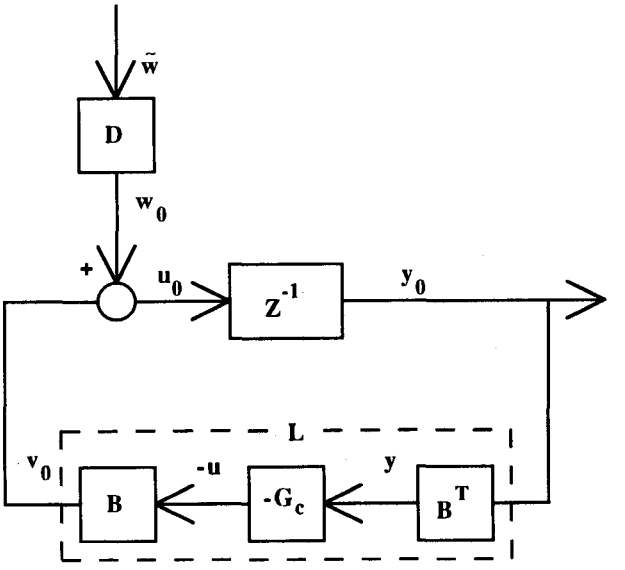

Fig. 5.1. Feedback Representation of Coupled Structural Modes.

Next we consider a realization of the feedback system in Fig. 5.1. The transfer functions $Z^{-1}(s)$ and $G_{\mathrm{c}}(s)$ are expressed by the state space models

$$\dot{x}(t) = Ax(t) + B_0u_0(t), \tag{49}$$

$$y_0(t) = B_0x(t), \tag{50}$$

$$\dot{x}_{\mathrm{c}}(t) = A_{\mathrm{c}}x_{\mathrm{c}}(t) + B_{\mathrm{c}}y(t), \tag{51}$$

$$u(t) = C_{\mathrm{c}}x_{\mathrm{c}}(t), \tag{52}$$

respectively. Since $u_0 = w_0 - v_0$ and $B_0B = B$, it follows from (40), (41) (49) - (52) that

$$\dot{x}(t) = Ax(t) + BC_{\mathrm{c}}x_{\mathrm{c}}(t) + B_0w_0(t), \tag{53}$$

$$\dot{x}_{\mathrm{c}}(t) = A_{\mathrm{c}}x_{\mathrm{c}}(t) + B_{\mathrm{c}}B^{\mathrm{T}}x(t). \tag{54}$$

Thus the feedback system (53) and (54) is given by

$$\dot{\tilde{x}}(t) = \tilde{A}\tilde{x}(t) + \tilde{D}\tilde{w}(t), \tag{55}$$

where

$$\tilde{x}(t) \triangleq \begin{bmatrix} x(t) \\ x_c(t) \end{bmatrix} \in \mathcal{R}^{4r}, \quad \tilde{A} \triangleq \begin{bmatrix} A & BC_c \\ B_c B^{\mathrm{T}} & A_c \end{bmatrix} \in \mathcal{R}^{4r \times 4r},$$

$$\tilde{D} \triangleq \begin{bmatrix} B_0 D \\ 0 \end{bmatrix} \in \mathcal{R}^{4r \times 2r}.$$

By setting $C = B^{\mathrm{T}}$ in (5), it can be seen that $\tilde{A}$ has the usual closed-loop structure.

Now we choose the performance variable in (30) to maximize energy flow from the ith structural mode, that is, to maximize $-P_i^{\mathrm{p}}$. By the same argument as in the previous section, this is equivalent to minimizing $-P_i^{\mathrm{d}}$. By defining

$$C_{1a} \triangleq [B_0 \quad 0_{2r \times 2r}] \in \mathcal{R}^{2r \times 4r}. \tag{56}$$

and

$$C_{\mathrm{da}} \triangleq \mathrm{diag}(0, 2\zeta_1\omega_1, 0, 2\zeta_2\omega_2, \ldots, 0, 2\zeta_r\omega_r), \tag{57}$$

then P_i^{d}, $i = 1, \ldots, r$, is given by

$$P_i^{\mathrm{d}} = -[C_{\mathrm{da}} C_{1a} \tilde{Q} C_{1a}^{\mathrm{T}}]_{(2i,2i)}, \tag{58}$$

where $\tilde{Q}$ satisfies the Lyapunov equation

$$0 = \tilde{A}\tilde{Q} + \tilde{Q}\tilde{A}^{\mathrm{T}} + \tilde{D}\tilde{D}^{\mathrm{T}}. \tag{59}$$

Thus the performance index to be minimized is given by

$$[C_{\mathrm{da}} C_{1a} \tilde{Q} C_{1a}^{\mathrm{T}}]_{(2i,2i)}$$

and in the similar manner as the previous section the performance matrix E_1 in (30) is given by

$$E_1 = \sqrt{2\zeta_i\omega_i}\, e_i^{\mathrm{T}} C_{1a}. \tag{60}$$

Finally, since (40) and (41) comprise a state space model of the structure given by (39), it follows that the plant (A, B, C) is strictly positive real. We can thus obtain a strictly positive real controller $-G_c(s)$ in the same manner as in the previous section.

As a numerical example, we now consider the simply supported uniform Bernoulli-Euler beam of length L in Fig. 5.2. The partial differential equation for the transverse deflection $\eta(\xi, t)$ is given by

$$\rho \frac{\partial^2 \eta(\xi,t)}{\partial t^2} + \frac{\partial^2}{\partial \xi^2}\left[EI_{\mathrm{A}} \frac{\partial^2 \eta(\xi,t)}{\partial \xi^2}\right] = \sum_{i=1}^{r} \delta(\xi - \xi_i) u_i(t) + \sum_{i=1}^{n} \delta(\xi - \xi_{\mathrm{d}i}) \tilde{w}_i(t). \tag{61}$$

with boundary conditions

$$\eta(\xi,t)|_{\xi=0,L} = 0, \quad EI_{\mathrm{A}} \frac{\partial^2 \eta(\xi,t)}{\partial \xi^2}|_{\xi=0,L} = 0,$$

where ρ is the mass per unit length, $\tilde{c}$ is the damping per unit length of the ith mode, EI_{A} is the bending stiffness.

By substituting (38) into (61) and using the orthogonality properties

$$\int_0^L \rho \psi_i(\xi)\psi_j(\xi) d\xi = \delta_{ij}, \quad \int_0^L EI_{\mathrm{A}} \frac{\partial^4}{\partial \xi^4} \psi_i(\xi)\psi_j(\xi) d\xi = \omega_i^2 \delta_{ij},$$

where δ_{ij} is the Kronecker delta, we obtain (39) with natural frequencies ω_i and eigenfunctions $\psi_i(\xi)$ given by

$$\omega_i = \sqrt{\frac{EI_{\mathrm{A}}}{\rho}} \left(\frac{i\pi}{L}\right)^2, \qquad \psi_i(\xi) = \sqrt{\frac{2}{\rho L}} \sin \frac{i\pi\xi}{L}, \quad i = 1, 2, 3, \ldots.$$

For numerical simplicity, let $L = \pi$ and $EI_{\mathrm{A}} = \rho = \frac{2}{\pi}$ so that

$$\omega_i = i^2, \qquad \psi_i(\xi) = \sin i\xi, \quad i = 1, 2, 3, \ldots.$$

Furthermore, two actuators are assumed to be located at $\xi_1 = 1, \xi_2 = 2$, and a white noise disturbance with unit intensity is entering at $\xi_{\mathrm{d}1} = 1.7$. Finally, we set $\zeta_1 = \zeta_2 = \zeta_3 = 0.01$ and $E_2 = I$ in (30) and retain the first three modes. The resulting energy flows are shown in Fig. 5.3 for controllers G_{c1}, G_{c2} and G_{c3} designed to maximize $-P_1^{\mathrm{p}}$, $-P_2^{\mathrm{p}}$ and $-P_3^{\mathrm{p}}$, respectively. These results show that each controller maximizes the energy flow from a specified mode and that the energy removed from each subsystem is dissipated by the coupling.

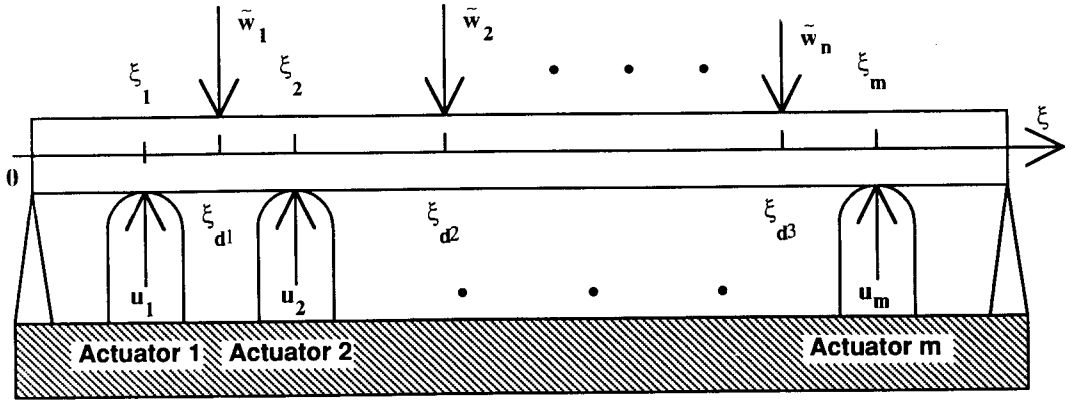

Fig. 5.2. Simply Supported Uniform Beam.

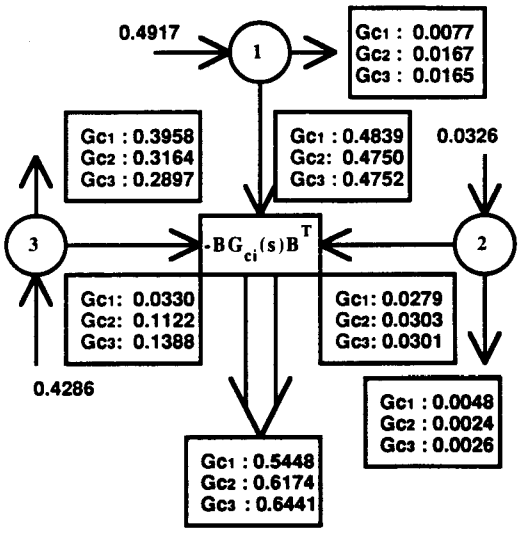

Fig. 5.3. Energy Flow among Structural Modes with Controllers.

Now we define the steady-state modal energy by

$$\mathcal{E}_i \triangleq \frac{1}{2}\mathcal{E}[\dot{q}_i^2(t)] + \frac{1}{2}\omega_i^2\mathcal{E}[q_i^2(t)], \quad i = 1,2,3, \tag{62}$$

and the result is shown in Table 5.1. Table 5.1 shows that controller G_{ci} successfully reduces the stored energy $\mathcal{E}_i$ of the ith mode.

Modal Energy	Open-Loop	Controller 1	Controller 2	Controller 3
$\mathcal{E}_1$	24.5847	0.3873 (1.58%)	0.8288 (3.37%)	0.8276 (3.37%)
$\mathcal{E}_2$	0.8160	0.0606 (7.43%)	0.0295 (3.17%)	0.0482 (5.91%)
$\mathcal{E}_3$	4.7618	2.1960 (46.12%)	1.7561 (36.88%)	1.3266 (27.86%)

Table 5.1. Steady-State Modal Energy of the ith Mode of a Flexible Beam.

6. Design of an Energy Flow Controller for Relative Force

As a further illustration of the approach of the previous section, we consider the interconnection of two positive real systems $z_i(s)$, $i = 1,2$, by means of a relative force controller. The controller thus serves as a dissipative coupling as in the previous section. This controller can be viewed as a device for regulating energy flow between two nominally uncoupled subsystems or as an interstitial device attached to two points on a single structure.

Let $Z^{-1}(s)$ and $G_c(s)$ represent the transfer functions of the two uncoupled strictly positive real systems and the controller, respectively, and assume these systems have the state space realizations

$$\dot{x}_p(t) = Ax_p(t) + B_p u_0(t), \tag{63}$$

$$y_0(t) = C_p x_p(t), \tag{64}$$

$$\dot{x}_c(t) = A_c x_c(t) + B_c y(t), \tag{65}$$

$$u(t) = C_c x_c(t), \tag{66}$$

respectively, where $x_p(t) \in \mathcal{R}^n$, $u(t) \in \mathcal{R}^2$, $x_c(t) \in \mathcal{R}^n$. Now $y_0(t) \in \mathcal{R}^2$ is the velocity vector of the two uncoupled systems and the scalars $y(t)$ and $u(t)$ represent the relative velocity and relative force, respectively.

To obtain the relative velocity $y(t)$ and the coupling force $v_0(t) \in \mathcal{R}^2$ we define $\tilde{B}$ as

$$\tilde{B} \triangleq \begin{bmatrix} 1 \\ -1 \end{bmatrix}, \tag{67}$$

so that $y(t) = \tilde{B}y_0(t)$ and $v_0(t) = -\tilde{B}u(t)$. With $\tilde{B}$ given by (67), the feedback system shown in Fig. 6.1 is equivalent to Fig. 2.1, where in Fig. 6.1, $L(s)$ is given by

$$L(s) \triangleq -\tilde{B}G_c(s)\tilde{B}^T. \tag{68}$$

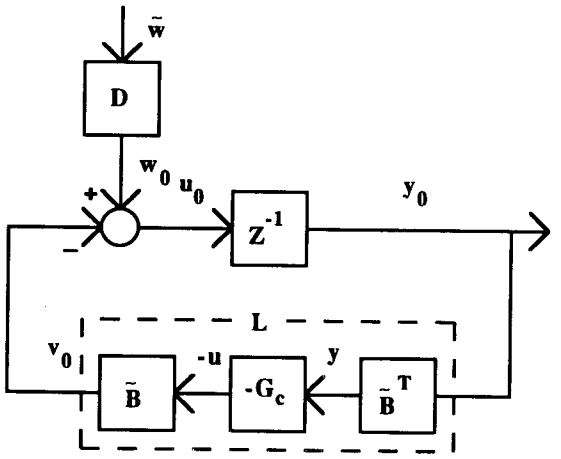

Fig. 6.1. Feedback Representation of Coupled System.

Thus the coupling $L(s)$ serves as a dissipative controller which controls energy flow between the subsystems.

Now (65) and (66) can be rewritten with $\tilde{B}$ as

$$\dot{x}_c(t) = A_c x_c(t) + B_c \tilde{B}^T y_0(t), \tag{69}$$

$$v_0(t) = -\tilde{B}C_c x_c(t). \tag{70}$$

Thus the feedback system (63), (64), (69) and (70) is given by

$$\dot{\tilde{x}}(t) = \tilde{A}\tilde{x}(t) + \tilde{D}\tilde{w}(t), \tag{71}$$

where

$$\tilde{x}(t) \triangleq \begin{bmatrix} x_p(t) \\ x_c(t) \end{bmatrix} \in \mathcal{R}^{2n}, \ \tilde{A} \triangleq \begin{bmatrix} A & B_p\tilde{B}C_c \\ B_c\tilde{B}^T C_p & A_c \end{bmatrix} \in \mathcal{R}^{2n\times 2n},$$

$$\tilde{D} \triangleq \begin{bmatrix} B_p D \\ 0 \end{bmatrix} \in \mathcal{R}^{2n\times 2}.$$

By setting $B = B_p\tilde{B}$ and $C = \tilde{B}^T C_p$, $\tilde{A}$ can be written as $\tilde{A} = \begin{bmatrix} A & BC_c \\ B_cC & A_c \end{bmatrix}$ so that (71) has the usual closed-loop structure.

Now we choose the performance variable $E_1x(t)$ to maximize the energy flow from the ith subsystem, where $i = 1, 2$. By the same argument in the previous sections this is equivalent to minimizing $-P_i^d$.

Define the 2×2 damping matrix C_{d1} by

$$C_{d1} \triangleq \text{diag}[c_1, c_2], \tag{72}$$

where $c_i \triangleq \text{Re}[z_i(s)]$, $i = 1, 2$. Then P_i^d, $i = 1, 2$, is given by

$$P_i^d = -[C_{d1}C_{pa}\tilde{Q}C_{pa}^T]_{(i,i)}, \tag{73}$$

where $C_{pa} \triangleq [C_p \ 0] \in \mathcal{R}^{2\times 2n}$, and $\tilde{Q}$ satisfies the Lyapunov equation

$$0 = \tilde{A}\tilde{Q} + \tilde{Q}\tilde{A}^T + \tilde{D}\tilde{D}^T. \tag{74}$$

Thus the performance matrix E_1 in (30) is given by

$$E_1 = \sqrt{c_i}e_i^T C_{pa}. \tag{75}$$

Since the plant represented by (A, B, C) is strictly positive real, we can use the positive real control approach to obtain the strictly positive real controller $-G_c(s)$.

To illustrate this approach we consider the two oscillator system with the coupling $L(s)$ shown in Fig. 6.2, where f represents the relative force. For illustrative purposes we set $k_1 = 10$, $k_2 = 2$, $m_1 = 0.3$, $m_2 = 0.4$, and $c_1 = 0.1$, $c_2 = 0.2$, and let the white noise disturbances $w_i(t), i = 1, 2$, have unit intensity, that is, $D = I$. By setting $E_2 = 0.1$ in (30) we design the controllers G_{c1} and G_{c2} to maximize $-P_1^p$ and $-P_2^p$, respectively. The resulting energy flows shown in Fig. 6.3 show that each controller successfully removes energy from the specified subsystem by minimizing the dissipated energy flow out of the subsystem. The steady-state stored energy $\mathcal{E}_i$, $i = 1, 2$, defined by (37) is listed in Table 6.1, which shows that each controller successfully reduces the stored energy of the corresponding oscillator. Furthermore, the Bode plots of the controllers in Fig. 6.4 show that the controllers are strictly positive real.

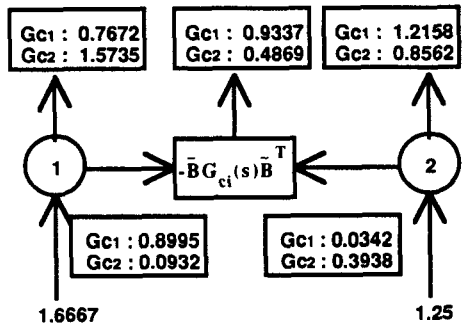

Fig. 6.3. Energy Flow between Oscillators with Controllers.

Stored Energy	Open-Loop	Controller 1	Controller 2
$\mathcal{E}_1$	5.0	2.6401 (52.08%)	4.5683 (91.37%)
$\mathcal{E}_2$	2.5	2.3549 (94.20%)	1.2041 (48.16%)

Table 6.1. Steady-State Stored Energy for Two Coupled Oscillators with Relative Force Actuator.

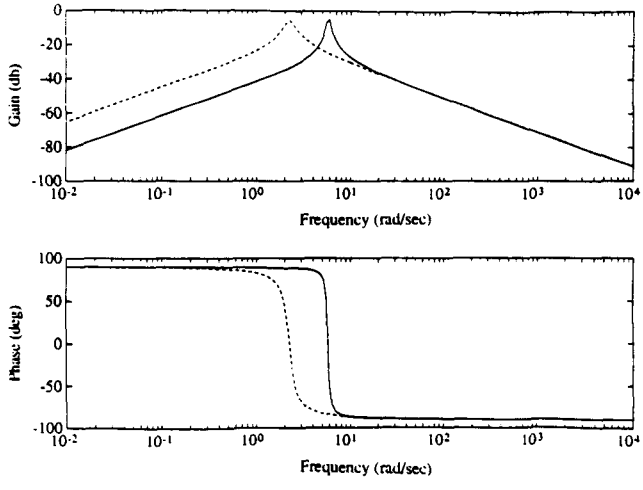

Fig. 6.4. Magnitude and Phase of Controllers G_{c1}(solid) and G_{c2}(dashed).

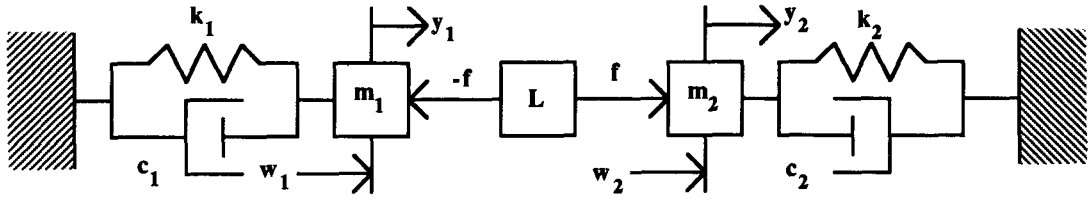

Fig. 6.2. Two Oscillator System with Relative Force Controller Coupling.

7. Conclusion

In this paper we applied energy flow models obtained in [7]-[9] to design energy flow controllers for modal subsystems. By using the LQG positive real control approach, each controller was considered as either an additional subsystem or as a dissipative coupling. Each resulting controller was shown to maximize energy flow from the specified subsystem. Furthermore, closed-loop asymptotic stability is guaranteed since strictly positive real controllers were designed in a negative feedback loop. These features were demonstrated by numerical examples.

Acknowledgments: This research was supported in part by the Air Force Office of Scientific Research under Grant F49620-92-J-0127 and the NASA SERC Grant NAGW-1335.

References

[1] Mace, B. R., "Active Control of Frexural Vibrations," *J. Sound Vib.*, Vol. 114, pp. 253-270, 1987.

[2] Von Flotow, A. H., and Shäfer, B. "Wave-Absorbing Controllers for a Flexible Beam," *J. Guid. Contr. Dyn.*, Vol. 9, pp. 673-680, 1986.

[3] Miller, D. W., Hall, S. R., and von Flotow, A. H., "Optimal Control of Power Flow at Structural Junctions," *J. Sound Vib.*, Vol. 140, No. 3, pp. 475-497, 1990.

[4] Pan, J., and Hansen, C. H., "Active Control of Total Vibratory Power Flow in a Beam. I: Physical System Analysis," *J. Acoust. Soc. Amer.*, Vol. 89, pp. 200-209, 1991.

[5] MacMartin, D. G., and Hall, S. R., "Control of Uncertain Structures Using an H_∞ Power Flow Approach," *J. Guid. Contr. Dyn.*, Vol. 14, pp. 521-530, 1991.

[6] MacMartin, D. G., and Hall, S. R., "Broadband Control of Flexible Structures using Statistical Energy Analysis Concepts," submitted to *J. Guid. Contr. Dyn.*

[7] Kishimoto, Y., and Bernstein, D. S., "Thermodynamic Modeling of Interconnected Systems: I. Conservative Coupling," submitted to *J. Sound Vib.*

[8] Kishimoto, Y., and Bernstein, D. S., "Thermodynamic Modeling of Interconnected Systems: II. Dissipative Coupling," submitted to *J. Sound Vib.*

[9] Wyatt, J. L., Siebert, W. M., and Tan, H. N., "A Frequency Domain Inequality for Stochastic Power Flow in Linear Networks," *IEEE Trans. Circ. Sys.*, Vol. 31, pp. 809-814, 1984.

[10] Lozano-Leal, R. and Joshi, S. M., "On the Design of Dissipative LQG-type Controllers," *Proc. IEEE Conf. Dec. Contr.*, Honolulu, HI, pp. 3492-3495, 1990.

[11] Benhabib, R. J., Iwens, R. P., and Jackson, R. L., "Stability of Large Structure Control Systems using Positivity Concepts," *J. Guid. Contr.*, Vol. 4, pp. 47-494, 1981.

[12] Anderson, B. D. O. and Vongpanitlerd, S., *Network Analysis and Synthesis: A Modern Systems Theory Approach*, Englewood Cliffs, NJ, Prentice-Hall, 1973.